# CHAPTER 9

# Hot Corrosion in Gas Turbines

## 9.1 Introduction

DURING COMBUSTION in the gas turbine, sulfur from the fuel reacts with sodium chloride from ingested air at elevated temperatures to form sodium sulfate. The sodium sulfate then deposits on the hot-section components, such as nozzle guide vanes and rotor blades, resulting in accelerated oxidation (or sulfidation) attack. This is commonly referred to as "hot corrosion."

Sulfur in the fuel is generally limited to 0.3% for commercial jet engines and to 1.0% for marine gas turbines (Ref 1). Sodium chloride comes from seawater (see Table 9.1) (Ref 2). Seawater is also a source of sulfur. For aircraft engines, Tschinkel (Ref 1) suggested that runway dust may be a source of salts.

Gas turbines generally use large amounts of excess air for combustion (a large fraction of air, in fact, is also used to cool the combustor), with a typical air-to-fuel ratio from about 40 to 1 (during takeoff) to 100 to 1 (at cruising speed) for aircraft gas turbine engines (Ref 2). These air-to-fuel ratios correspond to about 0.12 to 0.18 mole fractions of oxygen in the combustion zone (Ref 2). Thus, the combustion gas atmosphere is highly oxidizing. The sulfur partial pressure in the atmosphere can be extremely low, varying from $10^{-40}$ to $10^{-26}$ atm over the range from 330 to 1230 °C (620 to 2240 °F) (Ref 2). These sulfur partial pressures are well below those necessary to form chromium sulfides, which are frequently observed in alloys suffering hot corrosion attack.

High-temperature alloys that suffered hot corrosion attack were generally found to exhibit both oxidation and sulfidation. The hot corrosion morphology is typically characterized by a thick, porous layer of oxides with the underlying alloy matrix depleted in chromium, followed by internal chromium-rich sulfides. It is generally believed that the molten sodium sulfate deposit is required to initiate hot corrosion attack. The temperature range for hot corrosion attack, although dependent on alloy composition, is generally 800 to 950 °C (1470 to 1740 °F). The lower threshold temperature is believed to be the melting temperature of the salt deposit, and the upper temperature is the salt dew point (Ref 3). This type of corrosion process is sometimes referred to as Type I hot corrosion to differentiate it from Type II hot corrosion, which occurs at lower temperatures (typically 670 to 750 °C, or 1240 to 1380 °F) (Ref 4). Type II hot corrosion is characterized by pitting attack with little or no internal attack underneath the pit (Ref 4). Type II hot corrosion is rarely observed in aeroengines because the blades are generally operated at higher temperatures (Ref 5). However, marine and industrial gas turbines, which operate at lower temperatures, can experience low-temperature Type II hot corrosion.

Type I hot corrosion generally proceeds in two stages: an incubation period exhibiting a low corrosion rate, followed by accelerated corrosion attack. The incubation period is related to the formation of a protective oxide scale. Initiation of accelerated corrosion attack is believed to be related to the breakdown of the protective oxide scale. Many mechanisms have been proposed to explain accelerated corrosion attack; the salt fluxing model is probably the most widely accepted. Oxides can dissolve in $Na_2SO_4$ as anionic species (basic fluxing) or cationic species (acid fluxing), depending on the salt composition (Ref 6). Salt is acidic when it is high in $SO_3$, and basic when low in $SO_3$. The hot corrosion

**Table 9.1 Composition of seawater**

| Element | Composition, ppm |
|---|---|
| Chlorine | 18,980 |
| Sodium | 10,561 |
| Magnesium | 1,272 |
| Sulfur | 884 |
| Calcium | 400 |
| Potassium | 380 |
| Beryllium | 65 |

Source: Ref 2

mechanism by salt fluxing has been discussed in detail in Ref 7, 8, and 9. The topic of hot corrosion has been extensively covered in several reports and conference proceedings (Ref 2, 10–13).

## 9.2 Alloys Resistant to Hot Corrosion

Various test methods have been used to study hot corrosion. Immersion testing (or crucible testing), which was the first laboratory test method, is not considered reliable for simulating the gas turbine environment (Ref 14, 15). The salt-coated method is quite popular in academia for studying corrosion mechanisms. Engine manufacturers, however, use the burner rig test system to determine relative alloy performance ranking. The rig burns fuel with excess air to produce combustion gases with continuous injection of a synthetic sea-salt solution. This type of test system represents the best laboratory apparatus for simulating the gas turbine environment. A special issue of *High Temperature Technology* published in 1989 contained a number of papers discussing burner rig test procedures (Ref 16). The data reviewed here are limited to those generated by burner rig test systems.

### *9.2.1 High Temperature or Type I Hot Corrosion*

Bergman et al. (Ref 17) studied hot corrosion resistance of various nickel- and cobalt-base alloys at temperatures from 870 to 1040 °C (1600 to 1900 °F) with 5 ppm sea-salt injection. Their results are tabulated in Table 9.2. The data show a good correlation between alloy performance and chromium content. Increasing chromium in the alloy significantly improves resistance to hot corrosion. Alloys with 15% Cr or less are very susceptible to hot corrosion attack. Cobalt-base alloys are generally better than nickel-base alloys. This may simply be due to higher chromium contents in cobalt-base alloys. One nickel-base alloy (Hastelloy X) with a chromium level similar to those of cobalt-base alloys was found to behave similarly to cobalt-base alloys.

Among the alloys tested (Ref 17), alloy X-40 (Co-25Cr-10Ni-7.5W) performed best. This is in good agreement with the operating experience obtained by Royal Navy Ship (U.K.), which has demonstrated the superior hot corrosion resistance of alloy X-40 in a marine environment (Ref 18). Alloy X-40 was also found to be significantly better than nickel-base alloys (Ref 19), such as B-1900, U-700, U-500, and IN738 (Table 9.3). After 240 h, alloy X-40 showed hardly any corrosion attack, while alloy B-1900 (Ni-10Co-8Cr-6Mo-4.3Ta-6Al-1Ti) suffered severe attack. Alloy U-500 (Ni-18Co-19Cr-4Mo-2.9Al-2.9Ti) and IN738 (Ni-8.5Co-16Cr-1.7Mo-2.6W-1.7Ta-0.9Nb-3.4Al-3.4Ti) were similar, suffering only mild attack. Surprisingly, alloy U-700 (15% Cr) was found to be slightly worse than alloy B-1900 (8% Cr). Alloy B-1900 along with IN100 (10% Cr) and Nimonic 100 (11% Cr) were considered to be poor in hot corrosion and suggested that they not be considered for use without coatings, even in mildly corrosive environments (Ref 20).

Burner rig tests were conducted (Ref 21) using residual oil, containing 3% S and 325 ppm

**Table 9.2 Results of burner rig hot corrosion tests on nickel- and cobalt-base alloys**

| | | Loss in sample diameter, mm (mils) | | | |
|---|---|---|---|---|---|
| Alloy | Chromium content in alloy, % | 870 °C (1600 °F) 500 h | 950 °C (1750 °F) 1000 h | 980 °C (1800 °F) 1000 h | 1040 °C (1900 °F) 1000 h |
| SM-200 | 9.0 | 1.6 (64.4) | 3.3+ (130+) | … | … |
| IN100 | 10.0 | 3.3+ (130+) | 3.3+ (130+) | … | … |
| SEL-15 | 11.0 | 3.3+ (130+) | 3.3+ (130+) | … | … |
| IN713 | 13.0 | 3.3+ (130+) | 2.0+ (77+) | … | … |
| U-700 | 14.8 | 1.7+ (66+) | 1.6 (63.9) | … | … |
| SEL | 15.0 | 1.2 (45.8) | 1.3 (51.8) | 0.3 (11.4) | … |
| U-500 | 18.5 | 0.2 (7.6) | 0.8 (31.7) | 0.7 (29.3) | … |
| Rene 41 | 19.0 | 0.3 (10.3) | … | 0.8 (30.8) | |
| Hastelloy alloy X | 22.0 | … | 0.3 (12.0) | 0.4 (15.2) | … |
| L-605 (alloy 25) | 20.0 | … | 0.4 (15.3) | 0.3 (11.3) | 1.1 (41.9) |
| WI-52 | 21.0 | 0.5 (21.4) | 0.5 (18.2) | … | 1.9 (73.9) |
| MM-509 | 21.5 | … | 0.3 (10.9) | … | 0.8 (31.8) |
| SM-302 | 21.5 | 0.14 (5.4) | 0.3 (10.0) | … | 0.6 (23.1) |
| X-40 | 25.0 | 0.11 (4.2) | 0.3 (11.6) | … | 0.5 (18.5) |

Note: 5 ppm sea salt injection. Source: Ref 17

NaCl (equivalent to 5 ppm NaCl in air), at 870 °C (1600 °F) for 600 h on several cobalt-base alloys, which were X-45 (Co-25Cr-10Ni-7.5W), MAR-M302 (Co-21.5Cr-10W-9Ta-0.2Zr), MAR-M509 (Co-21.5Cr-10Ni-7W-3.5Ta-0.2T-0.5Zr), S-816 (Co-20Cr-20Ni-4W-4Nb-4Mo), FSX-418 (Co-30Cr-10Ni-7W-0.15Y), and FSX-414 (Co-30Cr-10Ni-7W). The test results are shown in Fig. 9.1. All six cobalt-base alloys with chromium varying from 20 to 30% suffered little corrosion attack (about 0.04 to 0.12 mm, or 0.002 to 0.005 in., or 2 to 5 mils). Under the same test condition, Udimet 700 (Ni-15Cr-18.5Co-5.2Mo-5.3Al-3.5T) suffered about 0.76 mm (0.03 in., or 30 mils) of attack (Ref 21). Figure 9.2 summarizes the data for a group of nickel- and cobalt-base alloys at 870 to 1040 °C (1600 to 1900 °F) (Ref 22). Alloy U-700 was found to be inferior to IN713 at 950 °C (1750 °F). This was contrary to field experience. Alloy U-700 has served most reliably in aircraft jet engines, whereas IN713 has suffered severe hot corrosion in many applications (Ref 22). The authors attributed the high corrosion rate of alloy U-700 to the low chromium content in this heat (i.e., 13.6% versus 15.0% for regular heats).

A systematic study was conducted (Ref 22) to determine the effects of alloying elements on hot corrosion resistance. In the Ni-10Co-15Cr-4Al-2Ti system, decreasing chromium from 25 to 10% resulted in increases in hot corrosion attack (Fig. 9.3). The data also suggest that decreasing aluminum while increasing titanium improves hot corrosion resistance. Furthermore, addition of 8% W to Ni-10Co-15Cr-4Al-2Ti alloy resulted in no apparent change in hot corrosion resistance. In binary and ternary alloy systems of nickel- and cobalt-base alloys, these authors further observed the effectiveness of chromium in improving hot corrosion resistance at 910, 950, and 1040 °C (1675, 1750, and 1900 °F) (Ref 22). Results are shown in Fig. 9.4.

**Table 9.3 Results of burner rig tests at 874 °C (1605 °F) for nickel- and cobalt-base alloys**

| Exposure time, h | Penetration depth, mm/1000 h (mils/1000 h) B-1900 | U-700 | U-500 | IN738 | X-40 |
|---|---|---|---|---|---|
| 100 | 2.8 (111) | … | … | … | … |
| 170 | 2.5 (97) | 3.3 (129) | 0.7 (29) | … | … |
| 240 | 2.1 (83) | … | 0.5 (20) | 0.9 (35) | Slight |

Note: Diesel fuel containing 1.0% S, 125 ppm Na, 15 ppm Mg, 4.8 ppm Ca, 4.1 ppm K, and 225 ppm Cl, air-to-fuel ratio was 50 : 1, and 100 h cycle. Source: Ref 19

In examining the effect of the third alloying element in Ni-Cr alloys, they found that (Ref 22):

- Tungsten (8%) showed little effect at 910 and 950 °C (1675 and 1750 °F), but a slightly detrimental effect at 1040 °C (1900 °F).
- Cobalt was only slightly beneficial.
- Molybdenum was detrimental at 1040 °C (1900 °F), but had little effect at lower temperatures.
- Titanium (5%) showed significant improvement at 1040 °C (1900 °F), but little effect at lower temperatures.
- Aluminum (8%) was detrimental, causing severe hot corrosion attack at 1040 °C (1900 °F).

For Co-25Cr alloys, the effect of the third alloying element was summarized as (Ref 22):

- Tungsten (8%) was detrimental at 1040 °C (1900 °F), with little effect at lower temperatures.

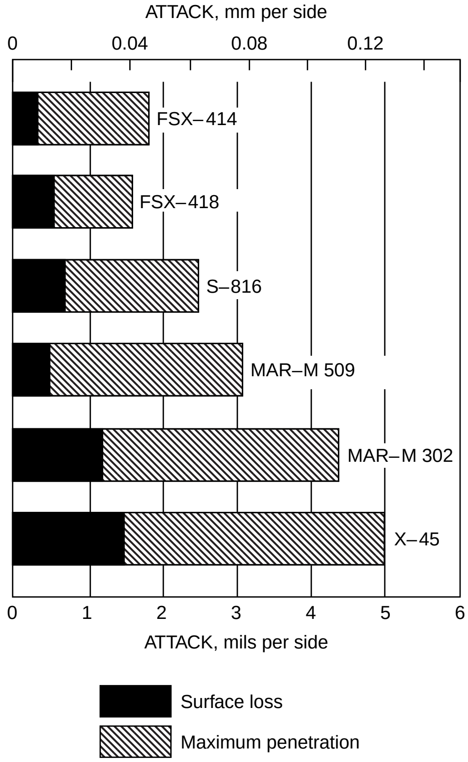

**Fig. 9.1** Relative hot corrosion resistance of cobalt-base alloys obtained from burner rig tests using 3% S residual oil and 325 ppm NaCl in fuel (equivalent to 5 ppm NaCl in air) at 870 °C (1600 °F) for 600 h. Source: Beltran (Ref 21)

- Molybdenum (6%) was detrimental at 950 and 1040 °C (1750 and 1900 °F), with little effect at 910 °C (1675 °F).
- Tantalum (7%) and nickel (10%) showed little effect.

Burner rig tests were conducted (Ref 23) at 900 °C (1650 °F) on several wrought superalloys and nickel aluminides. The combustion gas stream was generated by using No. 2 fuel oil containing about 0.4 wt% S with an air-to-fuel ratio of 35 to 1 and injection of either 5 or 50 ppm sea salt into the combustion gas stream. The specimens were loaded in a carousel, that rotated at 30 rpm during testing to ensure that all the specimens were subjected to the same test condition. The specimens were cycled out of the combustion gas stream once every hour for 2 min, during which time the specimens were cooled by forced air (fan cool) to less than 205 °C (400 °F). Superalloys tested were alloy X (Ni-22Cr-18.5Fe-9Mo-0.5W), alloy S (Ni-15.5Cr-14.5Mo-0.05La), alloy 230 (Ni-22Cr-14W-2Mo-0.02La), alloy 625 (Ni-21.5Cr-9Mo-3.6Nb), alloy 188 (Co-22Cr-22Ni-14W-0.04La), alloy 25 (Co-20Cr-10Ni-15W), and alloy 150 (Co-27Cr-18Fe). Two nickel aluminides, IC-50 (Ni-11.3Al-0.6Zr-0.02B) and IC-218

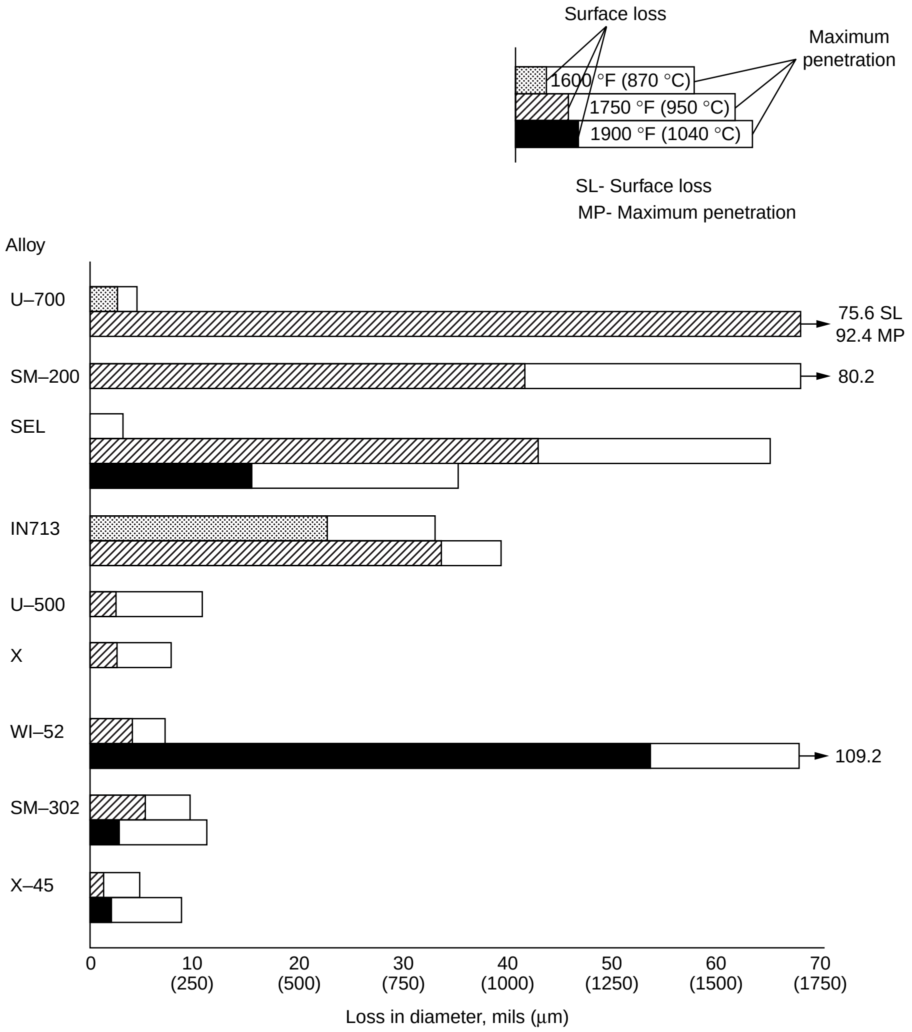

**Fig. 9.2** Relative hot corrosion resistance of nickel- and cobalt-base alloys obtained from burner rig tests at 870, 950, and 1040 °C (1600, 1750, and 1900 °F) for 100 h, using 1% S diesel fuel, 30:1 air-to-fuel ratio, and 200 ppm sea-salt injection. Source: Bergman et al. (Ref 22)

(Ni-7.8Cr-8.5Al-0.8Zr-0.02B), which were developed by Oak Ridge National Laboratory, were included in the test program.

The results of tests at 900 °C (1650 °F) for 200 h with 50 ppm sea salt are summarized in Table 9.4 (Ref 23). Both IC-50 and IC-218 nickel aluminides suffered severe hot corrosion attack after 200 h at 900 °C (1650 °F) with 50 ppm sea salt being injected into the combustion gas stream. Scanning electron microscopy with energy-dispersive x-ray spectroscopy (SEM/EDX) analysis showed that both nickel aluminides exhibited porous nickel or nickel-rich oxides with nickel sulfide penetrating through the remaining metal (Ref 23). Figure 9.5 shows the cross section of a corroded IC-218 specimen after hot corrosion burner rig testing at 900 °C (1650 °F) for 200 h with 50 ppm sea salt, revealing the formation of nickel oxides and nickel sulfides. SEM/EDX analysis showed that a thin, protective chromium-rich oxide scale formed on alloys X, 230, and 188.

Alloy 25, although exhibiting little weight change (Table 9.4), showed evidence of initial breakdown of the chromium-rich oxide scale. SEM/EDX analysis revealed the formation of cobalt-rich oxide nodules on the outer oxide scale on alloy 25. This indicated the initiation of the breakaway corrosion for alloy 25 after 200 h at 900 °C (1650 °F) with 50 ppm sea salt. Long-term test results under the same test condition clearly showed that alloy 25 suffered severe hot corrosion in excess of 200 h of testing, as shown in Fig. 9.6 (Ref 23).

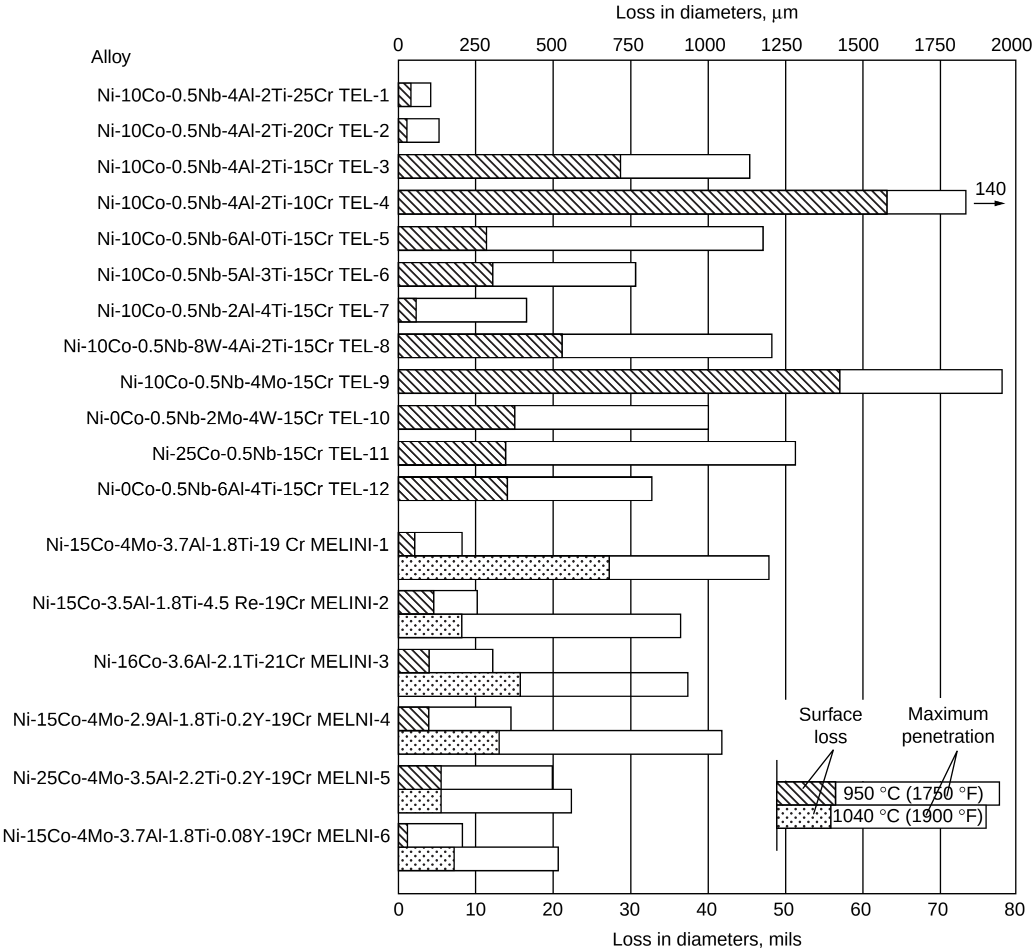

**Fig. 9.3** Relative hot corrosion resistance of experimental alloys obtained from burner rig tests at 950 and 1040 °C (1750 and 1900 °F) for 100 h, using 1% S diesel fuel, 30:1 air-to-fuel ratio, and 200 ppm sea-salt injection. Source: Bergman et al. (Ref 22)

Figure 9.6 also shows alloys 230 and 188 exhibiting very little weight change for exposure time up to 1000 h. The results of the 1000 h tests are summarized in Table 9.5 (Ref 23). Three nickel-base alloys (alloys S, X, and 625) and one cobalt-base alloy (alloy 25) were completely corroded before the test reached 1000 h, while nickel-base alloy 230 and cobalt-base alloys 150 and 188 exhibited little corrosion attack after 1000 h. Under the same test conditions in the same burner rig, nickel-base alloy HR-160 with 29% Co, 28% Cr and 2.75% Si was found to perform as well as alloys 230, 150, and 188. Figure 9.7 shows the conditions of the test specimens comparing HR-160 with other wrought alloys (Ref 24). Another burner rig test was conducted (Ref 23) with 5 ppm sea salt at 900 °C (1650 °F) under the same combustion conditions (i.e., No. 2 fuel oil with 0.4% S and 35-to-1 air-to-fuel ratio). The results are summarized in Table 9.6. Even at this low level of sea salt (5 ppm) in the combustion gas stream, cobalt-base alloy 25 continued to exhibit very poor hot corrosion resistance compared with some nickel-base alloys.

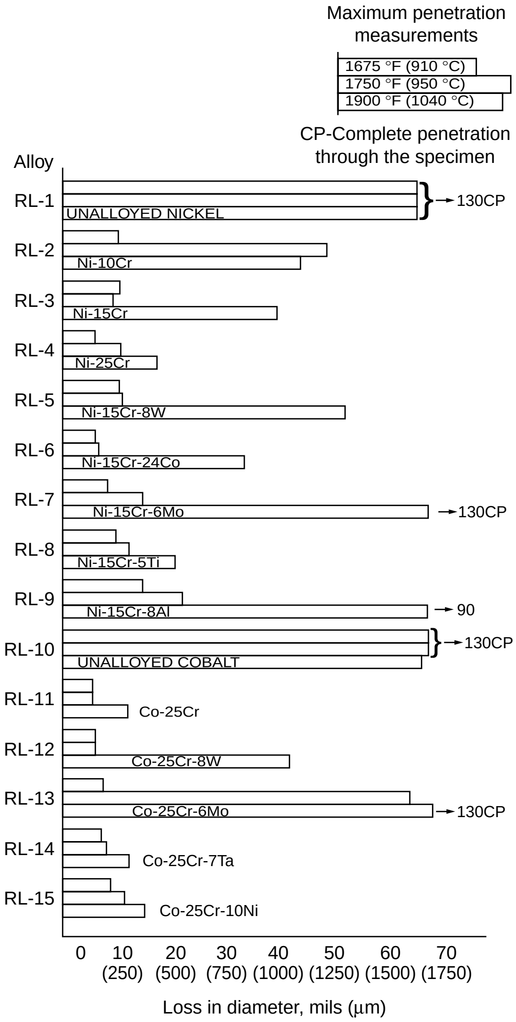

**Fig. 9.4** Relative hot corrosion resistance of experimental alloys obtained from burner rig tests at 910, 950, and 1040 °C (1675, 1750, and 1900 °F) for 100 h, using 1% S diesel fuel, 30:1 air-to-fuel ratio, and 200 ppm sea salt injection. Source: Bergman et al. (Ref 22)

### 9.2.2 Low-Temperature or Type II Hot Corrosion

"Low-temperature" or Type II hot corrosion has been observed at temperatures lower than the temperature range where Type I hot corrosion has been encountered. Severe hot corrosion of alloy S590 and Nimonic 80A after several thousand hours of operation in a gas turbine that burned blast-furnace gas with the 700 to 730 °C (1290 to 1345 °F) turbine entry temperature was reported in Ref 25. In 1976, a new form of hot corrosion attack of gas turbine airfoil materials in a marine gas turbine was reported (Ref 26). The first-stage turbine blades coated with a CoCrAlY coating, which had exhibited satisfactory hot corrosion resistance for metal temperatures in the range 800 to 1000 °C (1470 to 1830 °F), were found to suffer corrosion attack for metal temperatures at about 600 to 730 °C (1110 to 1345 °F) (Ref 26). The corrosion

**Table 9.4 Results of burner rig hot corrosion tests at 900 °C (1650 °F) for 200 h with 50 ppm sea salt with specimens being cycled once every hour**

| Alloy | Weight change, mg/cm$^2$ | Metal loss, mm (mils) | Total depth of attack(a), mm (mils) |
|---|---|---|---|
| X | −0.76 | 0.02 (0.6) | 0.07 (2.8) |
| 230 | −1.35 | 0.02 (0.8) | 0.06 (2.4) |
| 25 | −1.62 | 0.02 (0.9) | 0.07 (2.8) |
| 188 | 0.93 | 0.02 (0.7) | 0.04 (1.6) |
| IC-50 | 72 | >0.72 (28.3), completely corroded | >0.72 (28.3), completely corroded |
| IC-218 | 83 | >0.75 (29.5), completely corroded | >0.75 (29.5), completely corroded |

(a) Metal loss + internal penetration. Source: Ref 23

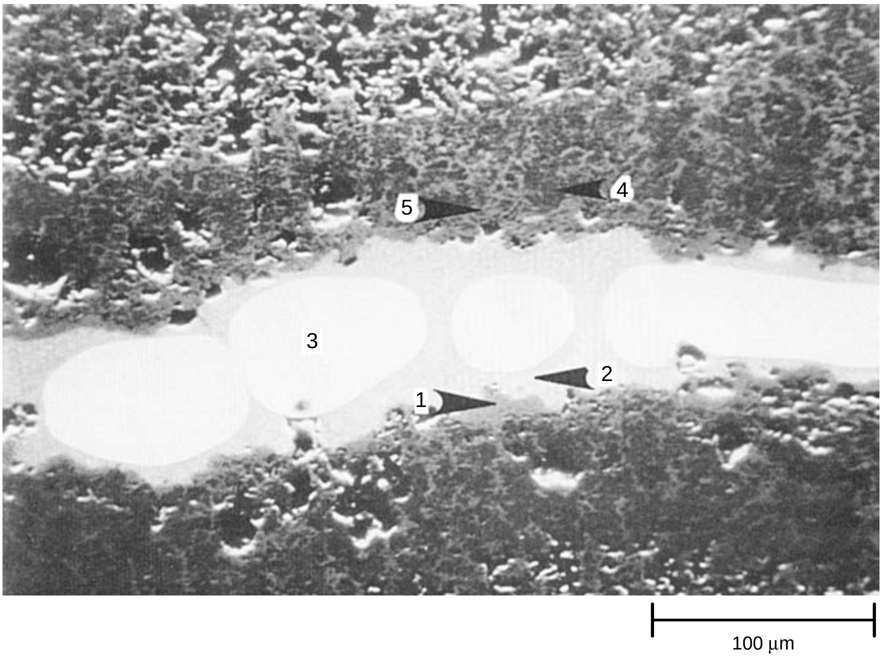

**Fig. 9.5** Scanning electron backscattered image showing the cross section of a corroded IC-218 nickel aluminide specimen after hot corrosion burner rig testing at 900 °C (1650 °F) for 200 h with 50 ppm sea salt using No. 2 fuel oil (0.4% S) for combustion at 35:1 air-to-fuel ratio. The results (wt%) of EDX analysis are: 1: 100% Ni; 2: 74% Ni, 26% S; 3: 100% Ni; 4: 88% Ni, 8% Cr, 4% Al; and 5: 98% Ni, 2% Al. Areas 1, 4, and 5 were essentially nickel oxides, area 2 was nickel sulfide, and area 3 was pure nickel. Courtesy of Haynes International, Inc.

products formed on the CoCrAlY coating were found to contain $CoSO_4$ and $NiSO_4$ (Ref 26). It was proposed (Ref 27) that the mechanism of low-temperature hot corrosion attack of a CoCrAlY coating involved the formation of the low melting $Na_2SO_4$-$CoSO_4$ eutectic (melting point of 565 °C, or 1045 °F). Nickel-base alloys were, in general, more resistant to Type II hot corrosion than cobalt-base alloys as found in Ref 28. It was also found (Ref 29) that NiCrAlY and NiCoCrAlY coatings were, in general, more resistant than CoCrAlY coatings.

Increases in chromium content in superalloys and coatings provided significant increases in low-temperature hot corrosion resistance (750 °C, or 1380 °F) for these materials (Ref 30). Both IN939 (23% Cr) and NiCrAlY coating (39% Cr) were found to exhibit good low-temperature hot corrosion resistance. NiCrAlY coatings with 26, 34, and 42% Cr were tested and found significant resistance to low-temperature hot corrosion for coatings with only 34 and 42% Cr (Ref 31). MCrAlY coatings (M = Co and/or Ni) with 30 to 35% Cr were tested (Ref 32). All of the coatings showed improved resistance to low-temperature hot corrosion (705 °C, or 1300 °F) compared with CoCrAlY coating with about 20% Cr. A critical chromium content of no less than 37% was required for cobalt-base coatings to provide resistance to both low- and high-temperature hot corrosion (Ref 33).

## 9.3 Summary

High-temperature or Type I hot corrosion generally occurs in the temperature range of 800 to 950 °C (1470 to 1740 °F). It is believed that the molten sodium sulfate deposit is required to initiate hot corrosion attack. The Type I hot corrosion morphology is typically characterized by a thick, porous layer of oxides with the underlying alloy matrix depleted in chromium, followed by internal chromium-rich sulfides. Low-temperature or Type II hot corrosion generally occurs in the temperature range of 670 to 750 °C (1238 to 1382 °F). Type II hot corrosion is characterized by pitting attack with little or no internal attack underneath the pit. Cobalt-base alloys are more susceptible to Type II hot corrosion, which generally involves

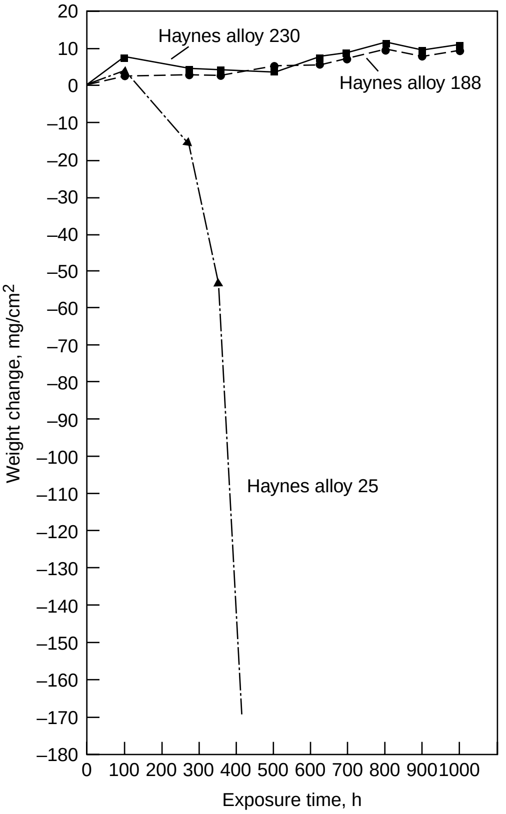

**Fig. 9.6** Results of burner rig tests at 900 °C (1650 °F) with 50 ppm sea salt using No. 2 fuel oil (0.4% S) for combustion at 35:1 air-to-fuel ratio for alloys 230, 188, and 25. Source: Lai et al. (Ref 23)

$Na_2SO_4$ and $CoSO_4$. Increasing chromium in alloys or coatings will improve the resistance of the material to both Type I and Type II hot corrosion attack.

**Table 9.5 Results of burner rig hot corrosion tests at 900 °C (1650 °F) for 1000 h with 50 ppm sea salt with specimens being cycled once every hour**

| Alloy | Weight change, mg/cm$^2$ | Total depth of attack(a), mm (mils) |
|---|---|---|
| S | ... | Completely corroded in 350 h (1.3 mm, or 49.2 mil thick specimen) |
| X | ... | Completely corroded in 500 h (1.2 mm, or 45.9 mil thick specimen) |
| 625 | ... | Completely corroded in 940 h (1.6 mm, or 63.7 mil thick specimen) |
| 230 | 11.5 | 0.11 (4.4) |
| 25 | ... | Completely corroded in 476 h (1.0 mm, or 37.8 mil thick specimen) |
| 150 | 10.0 | 0.13 (5.2) |
| 188 | 9.9 | 0.08 (3.2) |

(a) Metal loss + internal penetration. Source: Ref 23

## REFERENCES

1. J.G. Tschinkel, *Corrosion,* Vol 28 (No. 5), 1972, p 161
2. J. Stringer, "Hot Corrosion in Gas Turbines," Report MCIC-72-08, Battelle Columbus Laboratories, Columbus, OH, 1972
3. J. Stringer, *High Temperature Corrosion in Energy Systems,* M.F. Rothman, Ed., The Metallurgical Society of AIME, 1985, p 3
4. J. Stringer, Coatings in the Electricity Supply Industry: Past, Present, and Opportunities for the Future, *Surf. Coat. Technol.,* Vol 108/109, 1998, p 1
5. A.K. Koul, J.P. Immarigeon, R.V. Dainty, and P.C. Patnaik, Degradation of High Performance Aero-Engine Turbine Blades, *Advanced Materials and Coatings for Combustion Turbines,* V.P. Swaminathan and N.S. Cheruvu, Ed., ASM International, 1994, p 69
6. G.H. Meier, *High Temperature Corrosion 2 —Advanced Materials and Coatings* (Les Embiez, France), May 22–26, 1989, Elsevier Science, 1989, p 1
7. J.A. Goebel, F.S. Pettit, and G.W. Goward, *Metall. Trans.,* Vol 4, 1973, p 261
8. J. Stringer, *Am. Rev. Mater. Sci.,* Vol 7, 1977, p 477
9. R.A. Rapp, *Corrosion,* Vol 42 (No. 10), 1986, p 568
10. J. Stringer, R.I. Jaffee, and T.F. Kearns, Ed., *High Temperature Corrosion of Aerospace Alloys,* Advisory Group for Aerospace Research and Development, North Atlantic Treaty Organizations, AGARD-CP-120, Harford House, London, 1973
11. J.W. Fairbanks and I. Machlin, Ed., *Proc. 1974 Gas Turbine Materials in The Marine Environment Conf.,* MCIC-75-27, Battelle Columbus Laboratories, 1974
12. *Hot Corrosion Problems Associated with Gas Turbines,* STP 421, ASTM, 1967
13. A.B. Hart and A.J.B. Cutler, Ed., *Deposition and Corrosion in Gas Turbines,* Applied Science, London, 1973
14. J.F.G. Conde and G.C. Booth, *Deposition and Corrosion in Gas Turbines,* A.B. Hart and A.J.B. Cutler, Ed., John Wiley & Sons, 1973, p 278

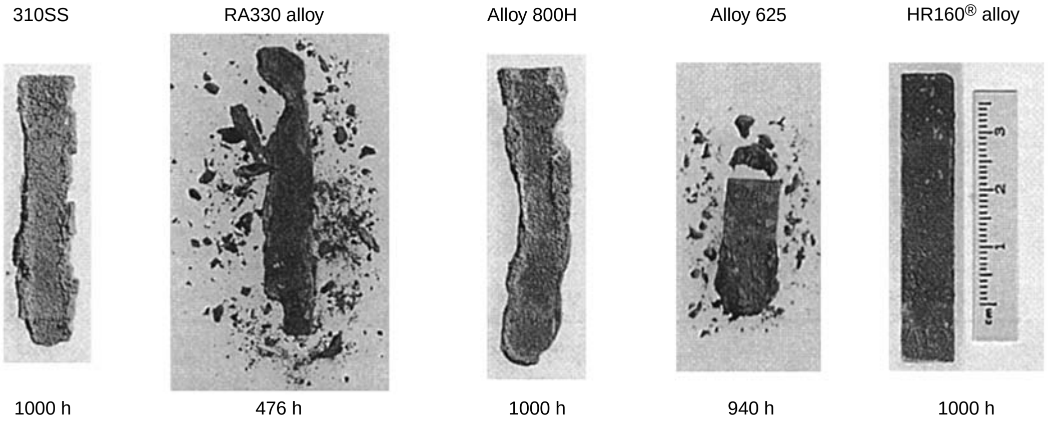

**Fig. 9.7** Test specimens alloy HR-160, 625, 800H, RA330, and Type 310 at 900 °C (1650 °F) in the combustion gas stream generated by a burner rig using No. 2 fuel oil (0.4% S) for combustion at 35:1 air-to-fuel ratio and with injection of 50 ppm sea salt into the combustion gas stream. During testing, specimens were cycled once every hour. Source: Ref 24

**Table 9.6 Results of burner rig hot corrosion tests at 900 °C (1650 °F) for 1000 h with 5 ppm sea salt with specimens being cycled once every hour**

| Alloy | Weight change, mg/cm$^2$ | Metal loss, mm (mils) | Total depth of attack(a), mm (mils) |
|---|---|---|---|
| X | −0.24 | 0.04 (1.6) | 0.14 (5.5) |
| 230 | −0.79 | 0.03 (1.2) | 0.13 (5.1) |
| 625 | 5.87 | 0.05 (1.9) | 0.14 (5.3) |
| 25 | … | … | Completely corroded (1.09 mm, or 43 mils) |
| 188 | 1.09 | 0.02 (0.8) | 0.07 (2.8) |

(a) Metal loss + internal penetration. Source: Ref 23

15. M.J. Donachie, R.A. Sprague, R.N. Russell, K.G. Boll, and E.F. Bradley, *Hot Corrosion Problems Associated with Gas Turbines,* STP 421, ASTM, 1967, p 85
16. *High Temperature Technology,* Special Issue on Hot-Salt Corrosion Standards Test Procedures and Performance, Vol 7 (No. 4), Nov 1989
17. P.A. Bergman, A.M. Beltran, and C.T. Sims, Development of Hot Corrosion-Resistant Alloys for Marine Gas Turbine Service, Final Summary Report to Marine Engineering Lab., Contract N600 (61533) 65661, Navy Ship R&D Center, Annapolis, MD, Oct 1, 1967
18. J. Clelland, A.F. Taylor, and L. Wortley, *Proc. 1974 Gas Turbine Materials in the Marine Environment Conf.,* MCIC-75-27, J.W. Fairbanks and I. Machlin, Ed., Battelle Columbus Laboratories, 1974, p 397
19. M.J. Zetlmeisl, D.F. Laurence, and K.J. McCarthy, *Mater. Perform.,* June 1984, p 41
20. J. Stringer, *Proc. Symp. Properties of High Temperature Alloys with Emphasis on Environmental Effects,* Z.A. Foroulis and F.S. Pettit, Ed., The Electrochemical Society, 1976, p 513
21. A.M. Beltran, *Cobalt,* Vol 46, 1970, p 3
22. P.A. Bergman, C.T. Sims, and A.M. Beltran, *Hot Corrosion Problems Associated with Gas Turbines,* STP 421, ASTM, 1967, p 38
23. G.Y. Lai, J.J. Barnes, and J.E. Barnes, "A Burner Rig Investigation of the Hot Corrosion Behavior of Several Wrought Superalloys and Intermetallics," Paper 91-GT-21, International Gas Turbine and Aeroengine Congress and Exposition (Orlando, FL), June 3–6, 1991
24. "Haynes HR-160 Alloy," H-3129A, Haynes International, Inc., Kokomo, IN
25. W. Moller, *Deposition and Corrosion in Gas Turbines,* A.B. Hart and A.J.B. Cutler, Ed., John Wiley and Sons, 1973, p 1
26. D.J. Wortman, R.E. Fryxell, and I.I. Bessen, A Theory for Accelerated Turbine Corrosion at Intermediate Temperatures, *Proc. Third Conference on Gas Turbine Materials in a Marine Environment,* Session V, Paper 11 (Bath, England), 1976
27. K.L. Luthra, *Metall. Trans. A,* Vol 13, 1982, p 1853
28. D.J. Wortman, R.E. Fryxell, K.L. Luthra, and P.A. Bergman, *Proc. Fourth US/UK Conf. on Gas Turbine Materials in a Marine*

*Environment* (Annapolis, MD), U.S. Naval Academy, 1979, p 317

29. L.F. Aprigliano, *Proc. Fourth US/UK Conf. on Gas Turbine Materials in a Marine Environment* (Annapolis, MD), U.S. Naval Academy, 1979, p 151
30. A.R. Taylor, B.A. Wareham, G.C. Booth, and J.F. Conde, Low and High Pressure Rig Evaluation of Materials and Coatings, *Proc. Third Conference on Gas Turbine Materials in a Marine Environment,* Session III, Paper No. 3 (Bath, England), 1976
31. J.F.G. Conde, G.C. Booth, A.F. Taylor, and C.G. McGreath, Hot Corrosion in Marine Gas Turbines, *Proc. Conf. High Temperature Alloys for Gas Turbines,* COST 50, 1982, p 237
32. J.A. Goebel, Advanced Coating Development for Industrial/Utility Gas Turbine Engines, *Proc. First Conf. on Advanced Materials for Alternative Fuel Capable Directly Fired Heat Engines* (Castine, ME), Department of Energy–Electric Power Research Institute, 1979, p 473
33. K.L. Luthra and J.H. Wood, High Chromium Cobalt-Base Coatings for Low Temperature Hot Corrosion, *Thin Solid Films,* Vol 119, 1984, p 271